Molecular Shapes, Orientation, and Packing of Polyoxometalate Arrays Imaged by Scanning Tunneling Microscopy

Mahmoud S. Kaba,[†] In K. Song,[†] Dean C. Duncan,[‡] Craig L. Hill,[‡] and Mark A. Barteau*[,†]

Center for Catalytic Science and Technology, Department of Chemical Engineering, University of Delaware, Newark, Delaware 19716, and Department of Chemistry, Emory University, Atlanta, Georgia 30322

Received May 14, 1997

Reported here are both STM images and spatially resolved tunneling spectra of four different polyoxometalate (POM) structural class members: Keggin structure, $H_3[PW_{12}O_{40}]$ (spherical); Finke−Droege (FD) structure, $Na_{16}[Cu_4(H_2O)_2(P_2W_{15}O_{56})_2]$ (prolate spheroidal); Wells−Dawson (WD) structure, $H_7[P_2Mo_{17}VO_{62}]$ (prolate spheroidal); and Pope−Jeannin−Preyssler (PJP) structure, $K_{12.5}Na_{1.5}[NaP_5W_{30}O_{110}]$ and $(NH_4)_{14}$ $[NaP_5W_{30}O_{110}]$ (oblate spheroidal). In all four cases, the results demonstrate the formation of well-ordered 2-D inorganic POM anion arrays (composed of catalytically active molecular constituents) on graphite. Importantly, the image shapes and lattice spacings accurately reflect the POM anisotropies, permitting the determination of anion orientation with respect to the surface plane.

Introduction

Although the scanning tunneling microscope is capable of atomic resolution imaging of solid surfaces, accurate imaging of adsorbates with even molecular resolution is far from routine. Successful molecular resolution imaging (i.e., images which yield accurate molecular shapes and sizes) has been demonstrated for various small organic molecules adsorbed and imaged in an ultrahigh-vacuum environment. Examples include mixed C_6H_6 and CO adlayers on Rh(111),[1] aromatics on Pt(111),[2] perylenetetracarboxylic acid on highly oriented pyrolytic graphite (HOPG),[3] and C_{60} on metal and semiconductor substrates.[4,5] In cases where the adsorbed layer is not close packed, the apparent molecular dimensions from such images may be distorted owing to adsorbate mobility, tip-dragging, and other effects.[6] Close-packed monolayers of a wide range of organics can be formed on surfaces by Langmuir−Blodgett and self-assembly techniques, for example, and accurate molecular resolution images (and, in some cases, images of intramolecular features) have been produced by STM under ambient conditions. Examples include alkanes, alkanethiols, alkyl aromatics, and liquid crystals,[7−11] as well as several organometallic complexes.[12,13]

The distinguishing characteristics of this work are the self-assembly and molecular imaging of well-ordered inorganic anion monolayers. We have chosen a set of polyoxometalate anions (POMs) with distinctive shapes in order to test the ability of STM to resolve molecular anisotropies of inorganic complexes under ambient conditions. POMs are d^0 early transition metal oxygen anion clusters which exhibit a wide diversity of molecular architectures, surface charge densities, and both photo- and thermoredox behaviors. These molecules have found applications as acid and oxidation catalysts,[14,15] electrode functionalization agents,[16] and antiretroviral agents.[17] One of the great advantages of POM monolayer assemblies as compared with the more widely studied organic monolayers is the greater thermal stability of POMs.[18] This stability makes monolayers of these discrete nanoscale clusters good candidates for catalytic and sensor applications which may require harsh environments.

Several groups have reported the formation of ordered arrays of POMs on surfaces and have imaged these using STM. Keita and Nadjo[19] deposited $H_3PW_{12}O_{40}$ from methanol solution by drying on HOPG, reporting resolution of individual anions in a periodic arrangement at the surface of the deposited layers. They suggested that their procedures produced "thin layers" which could not be "controlled to be uniformly spread as a monolayer" and noted difficulty in producing films giving images which permitted comparison with the known structure of $H_3PW_{12}O_{40}$.

* To whom correspondence should be addressed. Tel: (302) 831-8056. Fax: (302) 831-2085. E-mail: barteau@che.udel.edu.
[†] University of Delaware.
[‡] Emory University.

(1) Chiang, S.; Wilson, R. J.; Mate, C. M.; Ohtani, R. *J. Microsc.* **1988**, *152*, 567.
(2) Hallmark, V. M.; Chiang, S.; Meinhart, K.-P.; Hafner, K. *Phys. Rev. Lett.* **1993**, *70*, 3740.
(3) Ludwig, C.; Gompf, B.; Glatz, W.; Petersen, J.; Eisenmenger, W.; Möbus, M.; Zimmerman, V.; Karl, N. *Z. Phys. B* **1992**, *86*, 397.
(4) Altman, E. I.; Colton, R. J. *J. Vac. Sci. Technol. B* **1994**, *12*, 1906.
(5) Chen, D. M.; Xu, H.; Creager, W. N.; Burnett, P. *J. Vac. Sci. Technol. B* **1994**, *12*, 1910.
(6) Hallmark, V. M.; Chiang, S. *Surf. Sci.* **1993**, *286*, 190.
(7) Smith, D. P. E.; Hörbe, J. K. H.; Binnig, G.; Nejoh, H. *Nature* **1990**, *344*, 641.
(8) Rabe, J. P.; Buchholz, S. *Phys. Rev. Lett.* **1991**, *66*, 2096.
(9) Breen J. J.; Flynn, G. W. *J. Phys. Chem.* **1992**, *96*, 6825.
(10) Patrick, D. L.; Beebe, T. P. *Langmuir* **1994**, *10*, 298.
(11) Walba, D. M.; Stevens, F.; Parks, D.; Clark, N.; Wand, M. *Science* **1995**, *267*, 1144.
(12) Hudson, J. E.; Abruna, H. D. *J. Phys. Chem.* **1996**, *100*, 1036.
(13) Snyder, S. R.; White, H. S. *J. Phys. Chem.* **1995**, *99*, 5626.
(14) Misono, M. *Catal. Rev.—Sci. Eng.* **1987**, *29*, 269.
(15) Hill, C. L.; Prosser-McCartha, C. M. *Coord. Chem. Rev.* **1995**, *143*, 407.
(16) Keita, B.; Nadjo, L. *J. Electroanal. Chem.* **1990**, *287*, 149.
(17) Hill, C. L.; G.-S. Kim; C. M. Prosser-McCartha; Judd, D. In *Polyoxometalates: From Platonic Solids to Anti-retroviral Activity*; Pope, M. T., Muller, A., Eds.; Kluwer: Dordrecht, The Netherlands, 1993; p 359.
(18) Pope, M. T. *Heteropoly and Isopoly Oxometalates*; Springer-Verlag: New York, 1983.
(19) Keita, B.; Nadjo, L. *Surf. Sci.* **1991**, *254*, L443.

S0020-1669(97)00565-X CCC: $15.00
Published on Web 01/16/1998

Subsequent STM images of deposited $Na_6H_2[CeW_{10}O_{36}]\cdot 30H_2O$ from the same laboratory[20] were compared with AFM images of the bulk compound and were described as exhibiting short-range order owing to the uncontrolled nature of the deposition. Electrochemical deposition was suggested to give more uniform and reproducible thin films,[21] and it was noted that "thicker" regions of the POM deposits were difficult to image and exhibited considerable disorder.

Our initial report[22] provided the first evidence for the formation of POM monolayer arrays by depositing these compounds from solution onto HOPG by drying. Ordered arrays of the heteropolyanion derivatives $H_3PMo_{12}O_{40}$, $Na_4SiW_{12}O_{40}$, and $H_7SiW_9V_3O_{40}$, as well as the isopoly compound $(NH_4)_6V_{10}O_{28}\cdot 6H_2O$, were imaged. These ordered surface arrays exhibited periodicities consistent with the dimensions of the respective anions. Tunneling spectroscopy in air was applied to these materials for the first time, demonstrating (i) negative differential resistance in the spectra of all polyanions examined and (ii) the characteristic spectrum of graphite at the interstitial positions in the isopolyanion arrays, suggesting that the arrays imaged were indeed monolayers.[22] Recent work by Ge et al.[23] also demonstrated self-assembly of silicotungstate anion monolayers on a silver surface by electrochemical methods. Although the electronic states of the POMs which contribute to the STM images of these arrays have not been considered in detail, both the occupied and unoccupied frontier orbitals for the Keggin structure involve the 2p orbitals of the oxygen atoms at bridging positions in the framework.[24] The delocalization of the frontier orbitals over the Keggin framework may account for the absence of intramolecular features (i.e., the relatively isotropic appearance) for individual anions in surface arrays imaged by STM in these studies.

In several recent reports, we provided evidence both for the generality of ordered monolayer formation by POMs and for characteristics which distinguish arrays of different POMs.[25−28] We demonstrated that (i) a wide range of phosphomolybdate and phosphotungstate acids and their salts form ordered monolayers on graphite,[25−28] (ii) spatially resolved tunneling spectroscopy can distinguish the POMs from the graphite substrate observed at high-symmetry interstitial positions in these monolayers,[25−28] (iii) the lattice constants of these monolayers increase as the size of the countercations is increased,[25−28] (iv) NDR behavior is consistently observed in the tunneling spectra of individual polyanions in these arrays,[25−28] and (v) the NDR peak voltages correlate well with POM reduction potentials.[27,28]

In these previous STM investigations of POMs, measurements were recorded principally on members of the most common structural class—the Keggin structure.[29] We report here for the first time both STM images and tunneling spectra of members of four POM structural classes: Keggin,[29] $H_3[PW_{12}O_{40}]$; Finke−Droege[30] (FD), $Na_{16}[Cu_4(H_2O)_2(P_2W_{15}O_{56})_2]$; Wells−Dawson[31] (WD), $H_7[P_2Mo_{17}VO_{62}]$; and Pope−Jeannin−Preyssler[32] (PJP), $K_{12.5}Na_{1.5}[NaP_5W_{30}O_{110}]$ and $(NH_4)_{14}[NaP_5W_{30}O_{110}]$. Figure 1 shows spatially accurate structural representations of each class reconstructed from published X-ray crystal structures.[32−35] As shown below, all four POMs form well-ordered 2-D anion arrays on HOPG and, most importantly, their STM images accurately reflect the shapes and sizes characteristic of their respective structural classes, permitting the orientation of anisotropic POMs with respect to the surface plane to be determined.

Experimental Section

The POMs, $H_3[PW_{12}O_{40}]$, $K_{12.5}Na_{1.5}[NaP_5W_{30}O_{110}]$, $(NH_4)_{14}[NaP_5W_{30}O_{110}]$, and $Na_{16}[Cu_4(P_2W_{15}O_{56})_2]$, were prepared according to published procedures.[30,36−38] The WD complex, $H_7P_2Mo_{17}VO_{62}$, was supplied by the DuPont Co. (Wilmington, DE). The composition and structural integrity of the Keggin, PJP, and FD samples were verified by ^{31}P NMR and FTIR spectroscopy prior to use. The following chemical shifts (relative to 85% H_3PO_4 external standard) were measured by ^{31}P NMR: $H_3PW_{12}O_{40}$, −14.9 ppm (literature value −14.9 ppm[39]); $K_{12.5}Na_{1.5}[NaP_5W_{30}O_{110}]$, −10.4 ppm (literature values −10.35 ppm,[32] −9.9 ppm[40]). Infrared spectra obtained by deposition of the POMs on the diamond probe of a total internal reflectance FTIR spectrometer, described previously,[26] are given in the Supporting Information.

Samples for STM imaging were prepared by depositing one drop of aqueous POM solution (0.01 M) onto a freshly cleaved highly oriented pyrolytic graphite (HOPG) surface. The films were allowed to dry for 1 h under ambient conditions with the exception of the PJP sample which required vacuum desiccation to minimize bulk crystal formation. The images were acquired with a TopoMetrix TMX 2010 STM instrument either in air or in a N_2-filled glovebox. Sharp STM tips were prepared by cutting 90/10 Pt/Ir wire with sharp scissors. POM images were recorded with tips which first demonstrated both reproducible atomic resolution images of HOPG and 2-D fast Fourier transform (FFT) derived periodicities consistent with the standard value for graphite. All STM images were recorded with a sample bias of +100 mV and a tunneling current of 1−2 nA in the constant-current mode. The reported periodicities (lattice constants) of the 2-D images were obtained by 2-D FFT on several images acquired with at least three different tips and were calibrated against the periodicity measured for graphite with each individual tip. Post image processing (Fourier filtering) was performed only on the images of the Wells−Dawson (WD) and Finke−Droege (FD) samples.

Tunneling spectra for each POM sample were obtained with a minimum of three different tips; in each case, spectra were obtained at a number of positions in the corresponding STM image. Typical uncertainties in the positions of NDR peak voltages for POMs such as $H_3PW_{12}O_{40}$ and $Na_{16}[Cu_4(P_2W_{15}O_{56})_2]$ in this study, and others such as $H_3PMo_{12}O_{40}$ and $H_3PMo_9W_3O_{40}$ also examined,[41] were ±0.09 eV or less, obtained by sampling 24−40 spectra in each case.

(20) Keita, B.; Chauveau, F.; Theobald, F.; Belanger, D.; Nadjo, L. *Surf. Sci.* **1992**, *264*, 271.
(21) Keita, B.; Nadjo, L. *J. Electroanal. Chem.* **1993**, *354*, 295.
(22) Watson, B. A.; Barteau, M. A.; Haggerty, L.; Lenhoff, A. M.; Weber, R. S. *Langmuir* **1992**, *8*, 1145.
(23) Ge, M.; Zhong, B.; Klemperer, W. G.; Gewirth, A. A. *J. Am. Chem. Soc.* **1996**, *118*, 5812.
(24) Eguchi, K.; Seiyama, T.; Yamazoe, N.; Katsuki, S.; Taheta, H. *J. Catal.* **1988**, *111*, 336.
(25) Song, I. K.; Kaba, M. S.; Coulston, G.; Kourtakis, K.; Barteau, M. A. *Chem. Mater.* **1996**, *8*, 2352.
(26) Song, I. K.; Kaba, M. S.; Barteau, M. A. *J. Phys. Chem.* **1996**, *100*, 17528.
(27) Kaba, M. S.; Song, I. K.; Barteau, M. A. *J. Phys. Chem.* **1996**, *100*, 19577.
(28) Kaba, M. S.; Song, I. K.; Barteau, M. A. *J. Vac. Sci. Technol. A* **1997**, *15*, 1299.
(29) Keggin, J. F. *Nature* **1933**, *131*, 908.
(30) Finke, R. G.; Droege, M. W. *Inorg. Chem.* **1983**, *22*, 1006.
(31) Dawson, B. *Acta Crystallogr.* **1953**, *6*, 113.
(32) Alizadeh, M. H.; Harmalker, S. P.; Jeannin, Y.; Martin-Frere, J.; Pope, M. T. *J. Am. Chem. Soc.* **1985**, *107*, 2662.
(33) Brown, G. M.; Noe-Spirlet, M.-R.; Busing, W. R.; Levy, H. A. *Acta Crystallogr.* **1977**, *B33*, 1038.
(34) Weakley, T. J. R.; Finke, R. G. *Inorg. Chem.* **1990**, *29*, 1235.
(35) Strandberg, R. *Acta. Chem. Scand.* **1975**, *A29*, 350.
(36) Finke, R. G.; Droege, M. W.; Domaille, P. J. *Inorg. Chem.* **1987**, *26*, 3886.
(37) Wu, H. *J. Biol. Chem.* **1920**, *43*, 189.
(38) Preyssler, C. *Bull. Soc. Chim. Fr.* **1970**, 30.
(39) Massart, R.; Contant, R.; Fruchart, J.-M.; Ciabrani, J.-P.; Fourier, M. *Inorg. Chem.* **1997**, *16*, 2916.
(40) Kuwabara, M.; Clarke, D. R.; Smith, D. A. *Appl. Phys. Lett.* **1990**, *56*, 2396.
(41) Kaba, M. S. Ph.D. Dissertation, University of Delaware, 1998.

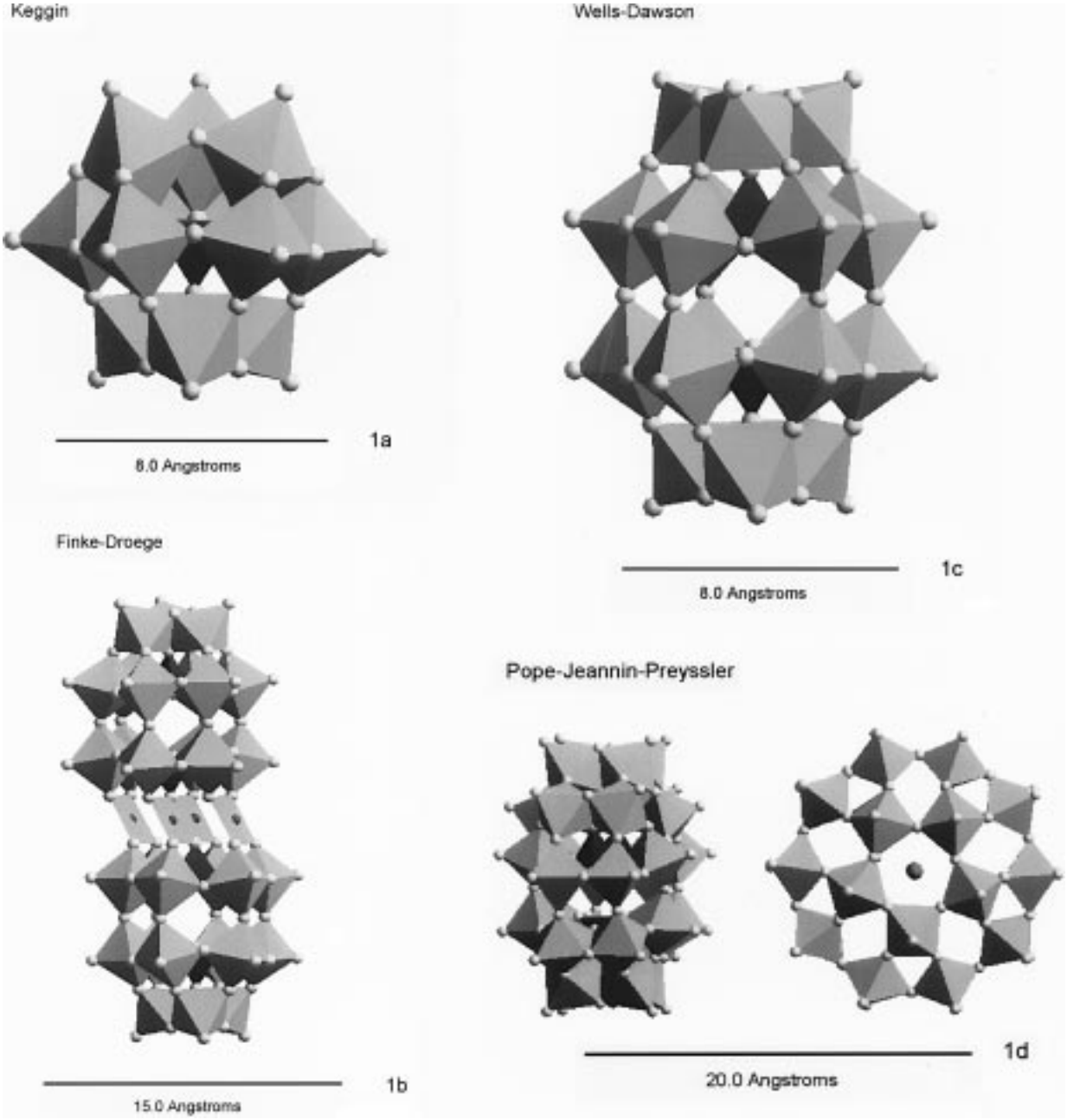

Figure 1. Accurate polyhedral representations of four polyoxometalate (POM) structural classes: (a) Keggin, $[PW_{12}O_{40}]^{3-}$; (b) Finke−Droege, $[Cu_4(H_2O)_2(P_2W_{15}O_{56})_2]^{16-}$; (c) Wells−Dawson, $[P_2Mo_{18}O_{62}]^{6-}$; (d) Pope−Jeannin−Preyssler, $[NaP_5W_{30}O_{110}]^{14-}$. The polyhedral vertices are occupied by oxygen and the polyhedral centers are occupied by P^V (tetrahedral) and Mo^{VI}, W^{VI}, or Cu^{II} (pseudooctahedral). These representations are constructed from atomic coordinates of published X-ray crystal structures using the Cerius[2] molecular simulation software package on a Silicon Graphics platform. The two views of the PJP anion depicted are (left) normal to the 5-fold axis and (right) along the 5-fold axis.

Results and Discussion

Uniformity of POM Layers. As noted by Keita and Nadjo,[19] deposition of POM layers by solvent evaporation may afford less control over array structure and thickness than do electrochemical methods. This expectation notwithstanding, we have found solvent evaporation to be a simple method to prepare ordered arrays of a wide variety of POMs on HOPG. In general, one observes the formation of a polycrystalline "rind" at the perimeter of the original droplet. Regions such as this in which crystallites are apparent to the naked eye or to a low power (×200) light microscope are insufficiently conductive to permit imaging by STM. The polycrystalline perimeter encloses a large region, typically several millimeters across, where the POM deposit is much thinner and where STM images of POM arrays can be reproducibly obtained. This region may exhibit crystalline inclusions and small multilayer patches, neither of which permits STM imaging owing to its low conductivity. Figure 2 shows a low-resolution AFM image characteristic of the interior region of the area originally covered by the solution of $H_3PW_{12}O_{40}$, after solvent evaporation. Most of the surface is quite flat (region C), but the presence of crystallites (regions labeled A) and of an additional layer deposit (region B) is evident. The latter is approximately 1−1.5 nm in height above the flat region of the surface, suggesting that it is one molecule thicker than the deposit in the flat regions. In this image, the flat portion of the surface extends for several microns, and it is not unusual to obtain AFM images of such samples with no topographic features in a flat planar area of 5 μm × 5 μm.

STM images of samples such as this exhibit ordered POM arrays over distances which are consistent only with the planar

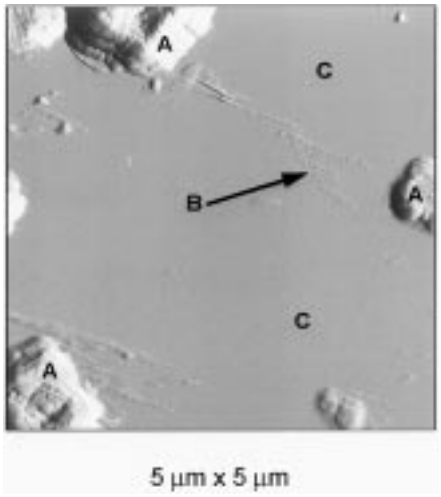

Figure 2. AFM image of $H_3PW_{12}O_{40}$ deposited on HOPG.

region of the AFM image. We have obtained molecular resolution STM images of molecularly flat POM arrays over regions as large as 1000 Å on a side. We have been unsuccessful in obtaining, within the regions originally covered by solvent, STM evidence for steps one molecule high, representing adjacent domains either of bare graphite and POM monolayers or of POM monolayers and multilayers. The inability to detect multilayer features above the plane of molecularly resolved POM arrays in STM suggests that deposits which are only two molecules in thickness may be insufficiently conductive to permit tunneling. Given our past demonstrations that the tunneling spectrum of graphite can be obtained at the high-symmetry interstitial positions of Keggin ion arrays,[25−27] we conclude that the deposits imaged with molecular resolution by STM are indeed one molecule in thickness. This is not to say that the solvent evaporation technique produces uniform monolayers; rather, those regions which are successfully imaged by STM and characterized as large arrays with uniform height and molecular resolution are monolayer deposits. As shown in Figure 2, such regions do in fact dominate the surface after solvent evaporation.

The Keggin Structure: $H_3[PW_{12}O_{40}]$. The approximately spherical Keggin structure (T_d symmetry) shown in Figure 1a[29,33] consists of a central PO_4^{3-} tetrahedron whose oxygen vertices are each linked to one of four W_3O_{13} groups. Each W_3O_{13} unit is composed of three WO_6 octahedra linked in a triangular arrangement by sharing edges, and the four W_3O_{13} groups are linked by sharing corners. Although the Keggin structure exhibits a high degree of symmetry, its polyhedral (rather than spherical) structure leads to some variation in its apparent diameter, depending upon the direction chosen. For example, if one assigns the standard ionic radius to the terminal oxo groups which define the perimeter of this structure, the Keggin anion $[PW_{12}O_{40}]^{3-}$, whose structure has been determined by X-ray diffraction (XRD),[33] can be completely contained in a cube 10.27 Å on a side, with its 2-fold axes of symmetry orthogonal to the cube faces. However, the van der Waals diameter along the 3-fold axis of symmetry (i.e., the vertical dimension of the structure depicted in Figure 1a) is 11.97 Å. One might therefore expect the packing of these units in either 2-D or 3-D lattices to exhibit intermolecular distances of similar magnitudes. Figure 3 shows an STM image of the Keggin anions deposited on HOPG. The image corrugations are spherical and form well-ordered 2-D arrays. The primitive unit cell is a rhombus with an included angle of 79.5° and a periodicity of 11.7 ± 0.3 Å as determined by fast Fourier

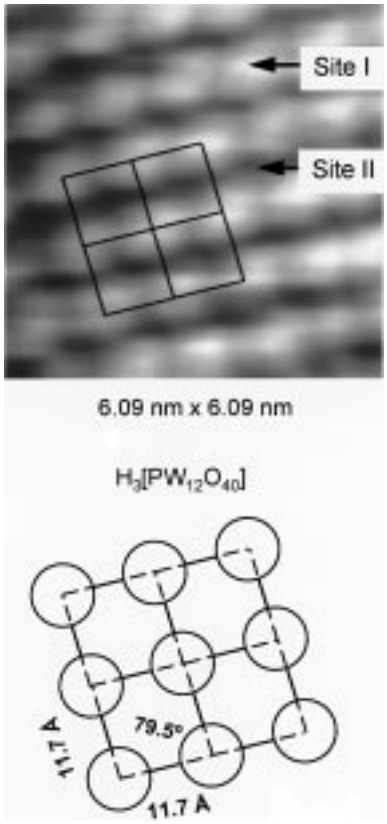

Figure 3. STM image and unit cell of the $H_3PW_{12}O_{40}$ array deposited on HOPG.

transform analysis of the image. We previously observed similar packing of other Keggin ion monolayers,[25] i.e., formally centered rectangular Bravais lattices; these are perhaps better thought of as minor distortions from square (in the present case) or hexagonal (e.g., for $Cs_3PMo_{12}O_{40}$[25]) packing. "Approximately square" packing of monolayer arrays of silicotungstate anions deposited on silver has also been reported by Ge et al.[23] In all of these cases both the shape and periodicity of the features observed by STM are consistent with the Keggin anion dimension derived from XRD. Further evidence that the corrugations in the images derive from discrete Keggin anions and not from graphite or Moiré anomalies[42,43] is obtained from tunneling spectroscopy (TS) measurements which are shown in Figure 4. Measured with the tip poised above a spherical corrugation (site I in Figure 3), the tunneling spectrum reveals an NDR peak at −1.20 V. In contrast, tunneling spectra measured at interstitial positions (site II in Figure 3) show no NDR behavior and are similar to the tunneling spectrum of HOPG. These TS results are once again consistent with a single-monolayer coverage of Keggin anions on the HOPG surface. This conclusion is in agreement with results for other members of the Keggin structural class, including $H_3PMo_{12}O_{40}$ and its alkali metal salts.[25−28]

It is instructive to compare the POM packing on the 2-D surface relative to that on the 3-D surface by comparing the structures of model STM images with particular cleavage planes of the bulk crystals. Model STM images were constructed (using Cerius[2] molecular simulation software) from both the lattice constants of the experimental STM images (determined

(42) Chang, H.; Bard, A. J. *Langmuir* **1991**, *7*, 1143.
(43) Winterlin, J.; Behm, R. J. In *Scanning Tunneling Microscopy I*; Guntherodt, H.-J., Wiesendanger, R., Eds.; Springer-Verlag: New York, 1992; p 50.

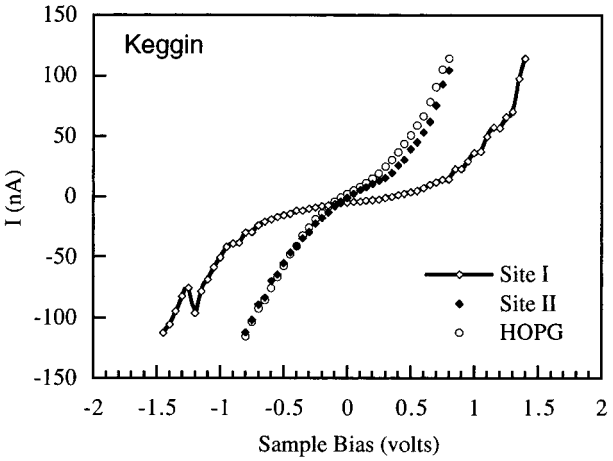

Figure 4. Spatially resolved tunneling spectra of the Keggin monolayer obtained at the sites indicated in Figure 3.

from 2-D fast Fourier transform (FFT) maps) and the POM van der Waals anion dimensions (determined from published X-ray crystal structures[33]). Figure 5 shows both a model STM image and the (100) plane of the Keggin bulk crystal. The tunneling spectra for the 2-D arrays suggest that the counterions are not located at the 4-fold hollow sites between anions. Results for monolayers of other Keggin salts employing larger countercations suggest that these cations occupy 2-fold bridge sites between pairs of anions,[25,26] as has also been proposed generically for bulk structures of these materials.[14] A comparison of the model STM image to the (100) plane of the bulk crystal indicates that the Keggin monolayer on HOPG exhibits similar symmetry but a smaller lattice spacing. This result is not surprising since the (100) plane (chosen to most closely match the planarity and symmetry of the 2-D array) is not the most close-packed plane in the structure. The nearest-neighbor (POM center-to-center) distance in the (100) plane is 12.51 Å, vs 10.83 Å in the most close-packed direction in the bulk.[33] The area per anion in the 2-D array in Figure 3 is 134.6 Å^2, approximately 14% less than the value for the (100) plane of the bulk structure. However, as we previously noted, the interstitial protons in bulk heteropolyacids are highly hydrated,[33] while the 2-D arrays imaged by STM show little evidence for water of crystallization.[25] It should also be recognized that most POM crystal structures do not consist of stacks of close-packed layers and typical cleavage planes are corrugated. It is therefore not surprising that the packing motif of POM arrays deposited on a flat surface does not necessarily reflect that of the most densely packed planes of the bulk structure. For monolayer structures, the absence of intermolecular interactions in the direction normal to the surface renders exact correspondence with bulk crystal planes unlikely. This notwithstanding, the conclusion to be drawn from Figure 5 is that there can be appreciable similarity between the monolayer and bulk packing for these compounds. In fact, for both the Keggin and the FD anions (as will be shown), a comparison of lattice periodicities between the 2-D and 3-D structures, coupled with spatially resolved tunneling spectra, permits the determination of countercation locations in the 2-D structures.

The Finke−Droege (FD) Structure: $Na_{16}[Cu_4(H_2O)_2(P_2W_{15}O_{56})_2]$. The prolate spheroidal structure (D_{2h} symmetry) is illustrated in Figure 1b[34,36] and consists of four planar edge-sharing $Cu^{II}O_6$ octahedra sandwiched between two α-$[P_2W_{15}O_{56}]^{12-}$ units. The latter units derive from the parent Wells−Dawson structure (vide infra) by the removal of three cap WO_6 octahedra. The calculated van der Waals anion

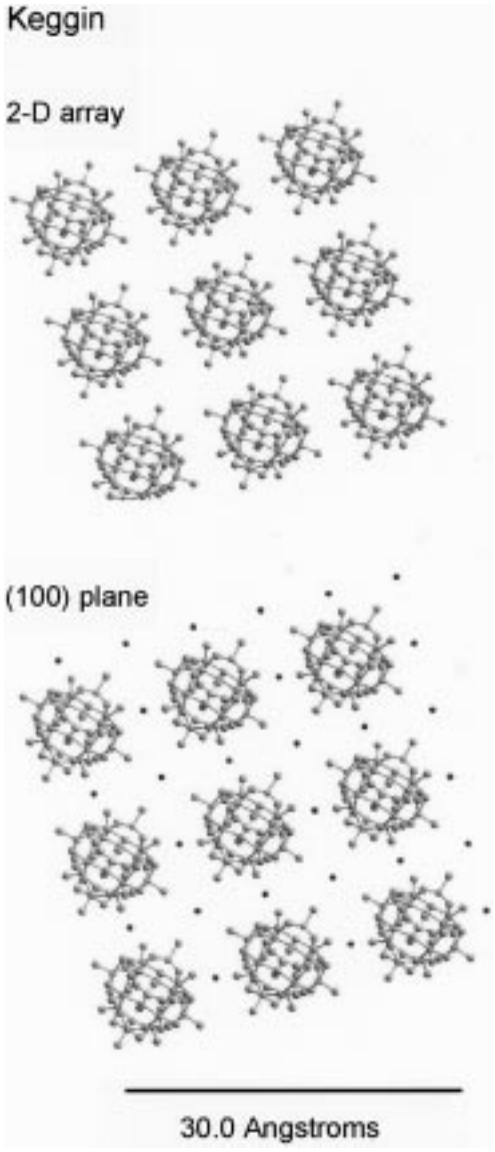

Figure 5. Comparison of Keggin anion packing between model STM images (see text) and the (100) plane of the 3-D crystal structure (derived from X-ray diffraction) of $H_3[PW_{12}O_{40}]\cdot 6H_2O$. Unattached (dark) spheres represent proton locations from XRD.[33]

diameters derived from XRD[34] for the minor and major axes of the structure depicted in Figure 1b are 11.69 and 24.21 Å, respectively. Figure 6 shows an STM image of the FD anion deposited on HOPG. The image shows well-ordered 2-D arrays. Both the primitive unit cell (rhombus) and the conventional unit cell (centered rectangle) are illustrated. The primitive cell has sides of 22.7 ± 0.4 Å with an included angle of 35.2°. As is apparent from examination of the conventional unit cell, the major axis of each of the prolate spheroidal molecules is aligned with the major axis of the rectangular cell. The minor axes are thus also aligned, with the minor axis of the rectangle having a length of 13.7 ± 0.2 Å. At first glance, the periodicities of the 2-D array may appear to be incompatible with the anion dimensions, but this difficulty is dispelled by comparison of the 2-D and 3-D structures. Figure 7 compares the model of the 2-D array from the STM image with the (100) plane of the bulk structure derived from XRD data.[34] The FD anion packings in the two structures are remarkably similar. The packing densities of the 2-D array and the bulk (100) plane in Figure 7 are also in agreement to within 8%, with the surface array slightly more densely packed (297.0 Å^2/anion vs 322.6 Å^2/anion

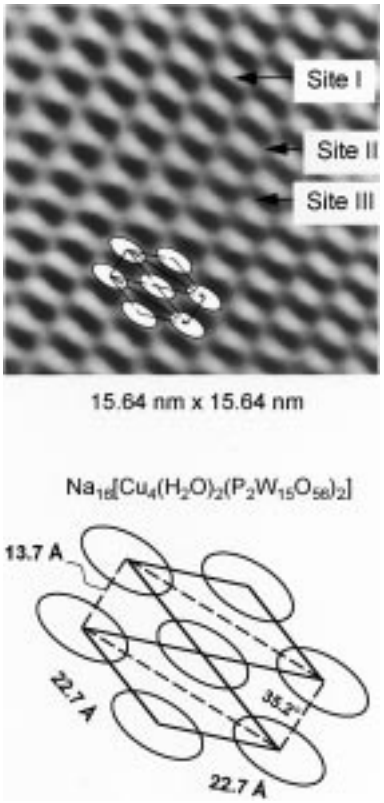

Figure 6. STM image and unit cell of the $Na_{16}[Cu_4(H_2O)_2(P_2W_{15}O_{56})_2]$ array on HOPG.

for the bulk (100) plane). In the (100) plane, the anions are packed in rows aligned along their minor axis; these rows are staggered with respect to each other, permitting the periodicity orthogonal to these rows to be slightly less (24.18 Å) than the length of the major axis of the anion. This same packing motif is apparent in the structure of the 2-D anion arrays in Figure 7 and suggests that the cation locations may also be similar to those in the (100) plane. In the bulk structure, the anions aligned in rows along their minor axis are separated by the Na^+ counterions which occupy the interstices in this direction. These counterions form a cylindrical "sheath" around the anion, with its axis collinear with the major axis of the anion. As a result, the interanion periodicity in the (100) plane along the minor axis is considerably larger than the van der Waals diameter of the anion along this axis (13.34 Å vs 11.69 Å). The excellent agreement of the anion periodicity in the 2-D arrays in this direction (13.7 ± 0.2 Å) with that of the bulk structure suggests that the countercations occupy similar positions in both cases.

This hypothesis can be tested by utilizing spatially resolved tunneling spectroscopy. Figure 8 shows tunneling spectra recorded at the three different sites indicated in the STM image (Figure 6). With the tip poised above a peak corrugation (site I), the tunneling spectra reproducibly (for sampling of >40 individual spectra) show NDR peaks at −0.80 ± 0.09 and +1.30 ± 0.05 V. Both the NDR and band-gap characteristics of the tunneling spectra at site I demonstrate that the images derive from FD anions and not from anomalies. As noted previously,[28] we have been unable to produce spectra exhibiting these features on bare graphite, even when imaging anomalies, e.g., Moiré fringes, have been observed. We have, however, demonstrated that POM monolayers consistently give rise to such tunneling spectra.[22,25−28] In contrast to the tunneling spectra obtained with the tip located above the anion, the spectrum measured between adjacent FD anions along the principal molecular axis (site II)

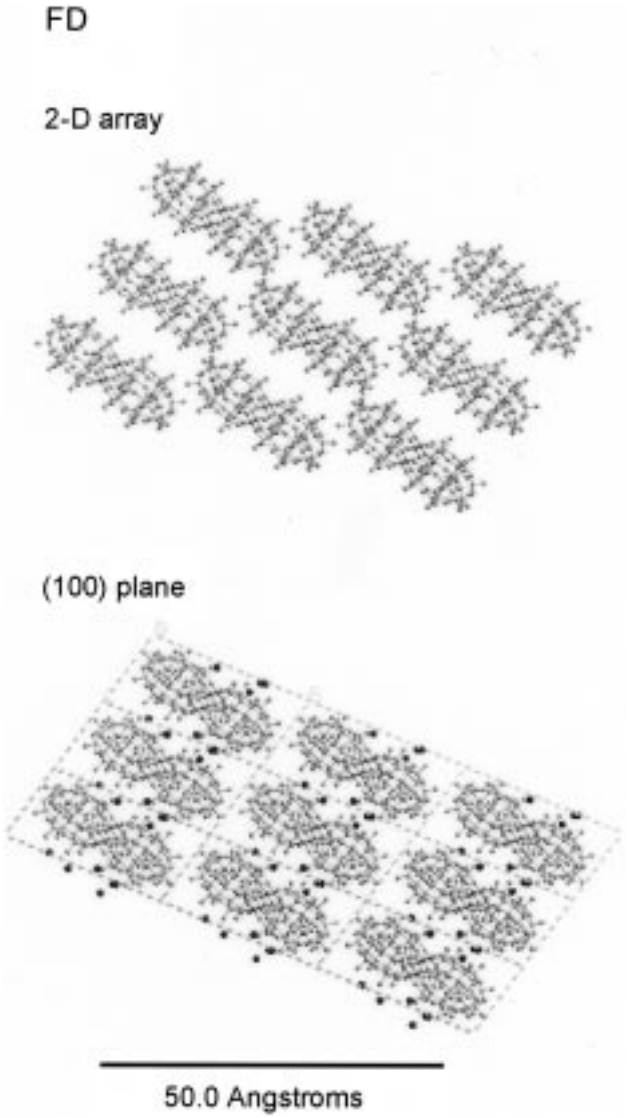

Figure 7. Comparison of FD anion packings between model STM images and the (100) plane of the bulk crystal, $Na_{16}[Cu_4(H_2O)_2(P_2W_{15}O_{56})_2]\cdot 53H_2O$. The largest (unattached) spheres in the crystal structure represent the positions of Na^+ countercations from XRD.[36] Positions of the water molecules are not shown.

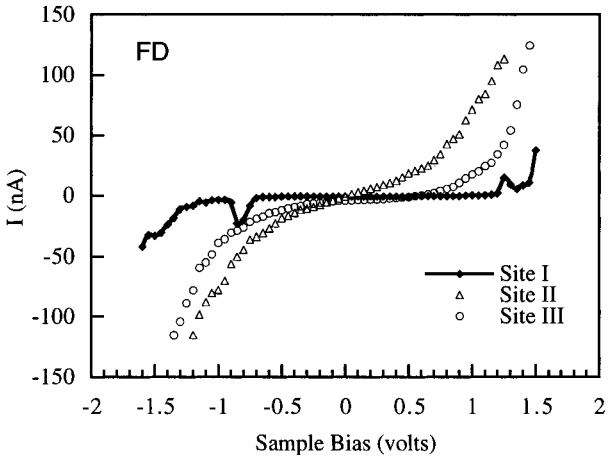

Figure 8. Spatially resolved tunneling spectra of the FD monolayer obtained at the sites indicated in Figure 6.

resembles that of the HOPG surface. It is not identical to that of HOPG shown in Figure 4; the smaller apparent gain in the spectrum at site II may simply reflect a spectrum obtained at

slightly greater sample-to-tip distances. However, this spectrum exhibits no electronic features which would distinguish this site from graphite. In contrast, the spectrum measured between adjacent FD anions perpendicular to the principal molecular axis (site III) is attributable neither to FD anions nor to the HOPG surface; the broad plateau is clear evidence for band-gap behavior. We tentatively attribute this spectrum to the presence of the countercations in this location, as inferred above from the correspondence of 2-D and 3-D structures. Ultraviolet photoelectron spectroscopy studies[43] show that adsorbate-related energy levels usually lie below the Fermi level; consequently, spectroscopic identification of adsorbed atoms or small molecules by STM is inherently difficult. Graphite is relatively inert, and minimal chemical interaction is expected between the adsorbates and graphite. Even so, the adsorbate-induced density-of-states (DOS) may exhibit a pronounced spatial and energetic structure. Tunneling spectroscopy probes the DOS a few angstroms above the surface. Since the spectra represent a convolution of both tip and sample properties, the spectral differences between sites within the POM monolayer and those on HOPG can result from modifications to either the tip or the sample. However, no significant differences were observed in either the tunneling spectra or STM images of native HOPG recorded both before and after measurements of the POM-derivatized surface. Consequently, the presence of an adsorbate on the tip during these measurements is highly unlikely. Similar observations were made in spectra/images recorded within a glovebox, suggesting that humidity also has little effect. We conclude that the spectra presented in Figure 8 represent three inequivalent but identifiable sites in the FD monolayer on HOPG.

The Wells−Dawson (WD) Structure: $H_7[P_2Mo_{17}VO_{62}]$. The prolate spheroidal WD structure (approximate D_3 symmetry) illustrated in Figure 1c consists of two defect Keggin A-type α-$[PM_9O_{34}]^{9-}$ (M = Mo^{VI} or W^{VI}) fragments which are linked by six nearly linear M−O−M bonds. The calculated minimum van der Waals anion diameters for the related α-$[P_2Mo_{18}O_{62}]^{6-}$ anion derived from a published X-ray structure determination[35] are 10.98 Å × 14.48 Å. The $(P_2Mo_{17}VO_{62})^{7-}$ anion is expected to have nearly identical dimensions. Figure 9 shows an STM image of the WD anion deposited on HOPG. The image shows well-ordered 2-D arrays. These exhibit oblique unit cells with sides of 13.1 ± 0.3 and 13.3 ± 0.3 Å (included angle = 47.4°). The distortion from centered rectangular packing is fairly small and, in fact, is within the uncertainty of the lattice dimensions determined by FFT analysis of the STM images. As for the FD anion, the WD anions are aligned in rows along their minor axes with an interanion separation of 10.3 Å in this direction. These rows are staggered with respect to each other, permitting a closer approach between rows than if the anions were packed end-to-end along their major axes. However, the lattice constants obtained for the 2-D arrays are slightly less than the values for related molecules from X-ray data and suggest that some interpenetration of the van der Waals dimensions of these anions may occur in the ordered arrays. Further comparison of these lattice constants and the corresponding packing densities with those observed in the bulk crystal structure is precluded by the different countercations used in each study. The observation of NDR in the tunneling spectra (not shown) in addition to the observed periodicities demonstrates that the image corrugations reflect the WD anion molecular topography.

The Pope−Jeannin−Preyssler (PJP) Structure: $K_{12.5}Na_{1.5}[NaP_5W_{30}O_{110}]$. The oblate spheroidal ($\sim D_{5h}$ symmetry) PJP structure illustrated in Figure 1d is constructed from five PW_6O_{22} units. Each PW_6O_{22} unit is structurally related to the Keggin anion, α-$[PW_{12}O_{40}]^{3-}$, by the removal of two sets each of three corner-shared WO_6 octahedra from α-$[PW_{12}O_{40}]^{3-}$. Five such PW_6O_{22} units are joined together in a pie-wedge fashion by the corner-sharing of their WO_6 octahedra to form an oblate spheroid. The van der Waals dimension determined from published XRD data[32] along the minor axis is 12.71 Å; the minimum dimension of the major axis is 16.70 Å (face-to-face) and 17.39 Å (corner-to-corner). Figure 10 shows an STM image of the PJP anions deposited on HOPG. The images form well-ordered 2-D arrays with periodicities of 18.6 ± 0.2 Å × 18.9 ± 0.2 Å (included angle = 41.2°). The anions are oriented with the 5-fold (minor) molecular axis parallel to the surface as illustrated schematically in Figure 11. Although the lattice in Figure 10 is formally oblique, it in fact represents a very slight distortion from a centered rectangular lattice. A distortion of the right angles of the rectangular unit cell by only 2° is required to reproduce the lattice in Figure 10; this is much smaller than, for example, the distortion from square symmetry of the lattice in Figure 3. As for the FD arrays, the anions in the PJP array in Figure 10 are arranged such that their principal axes are aligned with the axes of the rectangle (recognizing that the uncertainty in angular orientation is greater than the deviation from rectangular symmetry) as shown in Figure 11. Additionally, since the periodicities observed for these arrays, including the face-to-face separation between anions (13.2 Å), are larger than the van der Waals diameters determined by X-ray diffraction, they also likely reflect the presence of the countercations between the PJP anions in the 2-D array. Further evidence supporting this hypothesis is culled from TS measurements. Tunneling spectra obtained at the image corrugation peaks show NDR behavior at two applied voltages, −0.66 and +0.87 V, consistent with the assignment of these features to the PJP

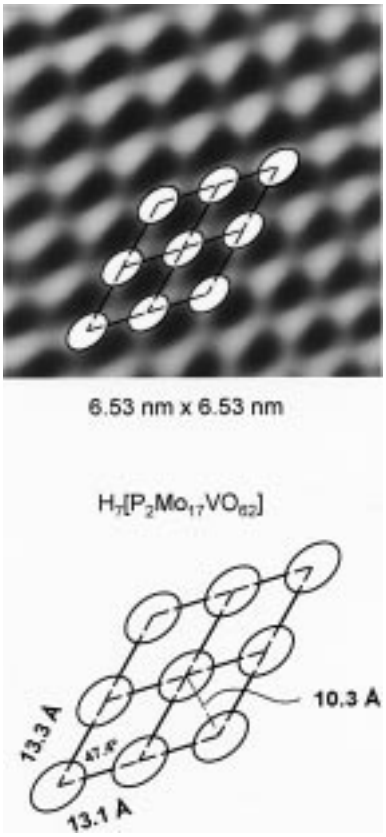

Figure 9. STM image and unit cell of the $H_7[P_2Mo_{17}VO_{62}]$ array on HOPG.

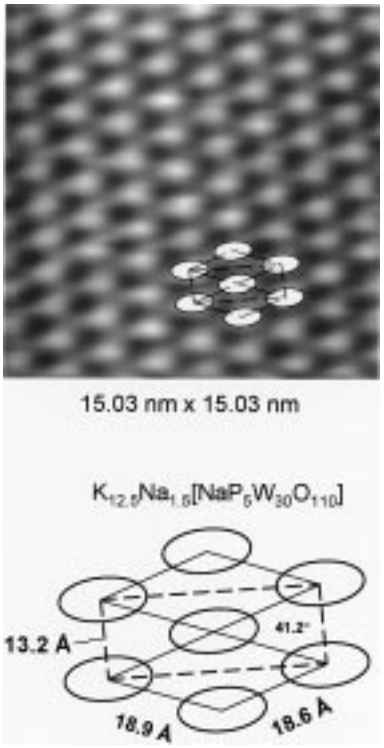

Figure 10. STM image and unit cell of the $K_{12.5}Na_{1.5}[NaP_5W_{30}O_{110}]$ array on HOPG.

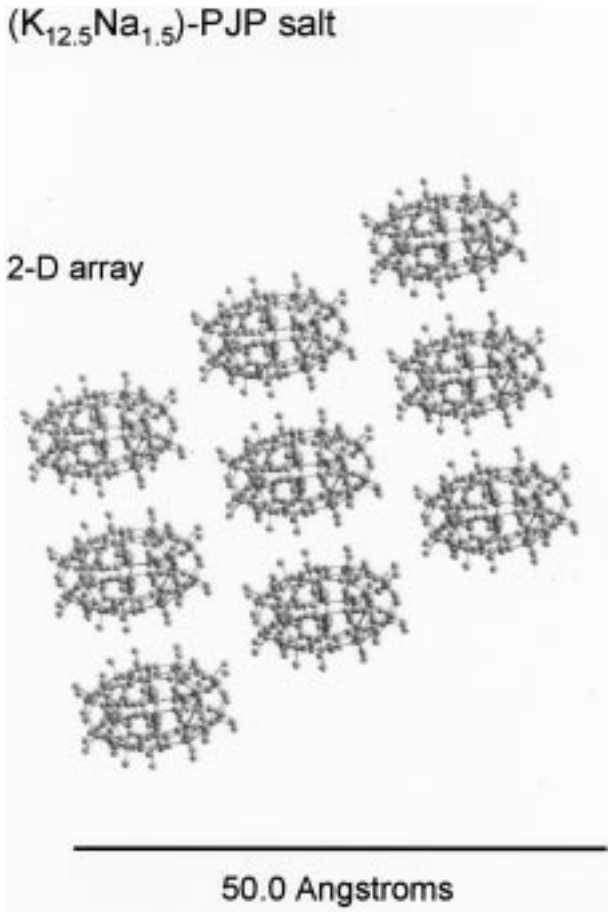

Figure 11. Model STM image of the $K_{12.5}Na_{1.5}$ PJP salt.

anions. Tunneling spectra at the interstitial spaces show no NDR behavior and are different from that of HOPG. Taken together, the tunneling spectra and the large lattice spacings both indicate the presence of the countercations at the interstitial spaces between the PJP anions. Further comparison of the lattice constants with those obtained from the bulk crystal structure is precluded by the different countercations used in each study. However, we have also performed STM on 2-D arrays of the same salt for which XRD results have been reported, $(NH_4)_{14}[NaP_5W_{30}O_{110}]$; a representative STM image is shown in Figure 12. The packing of molecules with the 2-D arrays of the NH_4 salt is similar to that of the alkali metal salt shown in Figure 10; the NH_4 PJP arrays are oblique with a periodicity of 13.8 ± 0.2 Å $\times$ 19.5 ± 0.2 Å (included angle = 56.9°). This lattice spacing, especially along the minor axis, compares favorably to that of the (010) plane of the bulk structure which exhibits the most similar anion arrangement (13.68 Å $\times$ 17.59 Å[32]). Relative to the potassium salt, it therefore appears that the larger NH_4^+ cation increases the lattice constant of the 2-D PJP arrays by 0.5 Å along the minor axis and 1 Å along the principal axis. The expansion along both axes is consistent with the relatively homogeneous distribution of the countercations around the anions in the bulk structure,[32] in contrast to the FD example presented above. Even more remarkable, however, is the influence of cation identity on the symmetry of the PJP anions arrays and on relationships to the 3-D crystal structure of the ammonium salt. Figure 13 illustrates the models constructed for the STM image of the ammonium PJP surface arrays along with the structure of the (010) plane of the crystal structure of the ammonium salt. In contrast to the surface arrays of the potassium salt, which can be described within experimental uncertainty as a centered rectangular lattice (Figures 10 and 11), the lattice for the ammonium PJP surface arrays is clearly oblique, as is the (010) plane of the bulk structure of the ammonium salt (Figure 13). Careful inspection of the model structures in Figures 11 and 13 reveal that the 5-fold axes of the anions in the surface arrays of the potassium

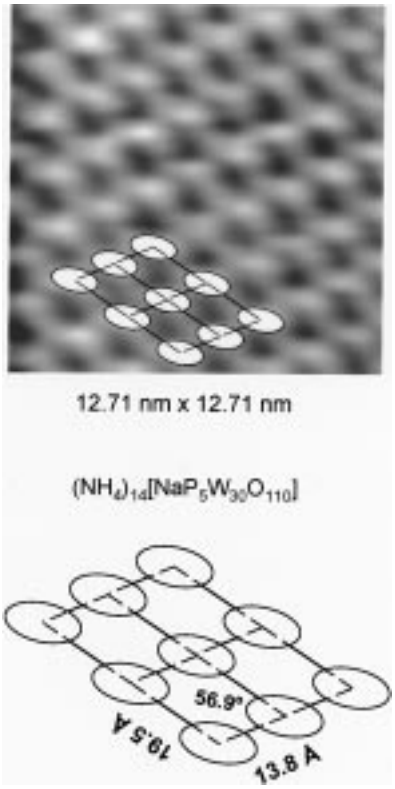

Figure 12. STM image and unit cell of the $(NH_4)_{14}[NaP_5W_{30}O_{110}]$ array on HOPG.

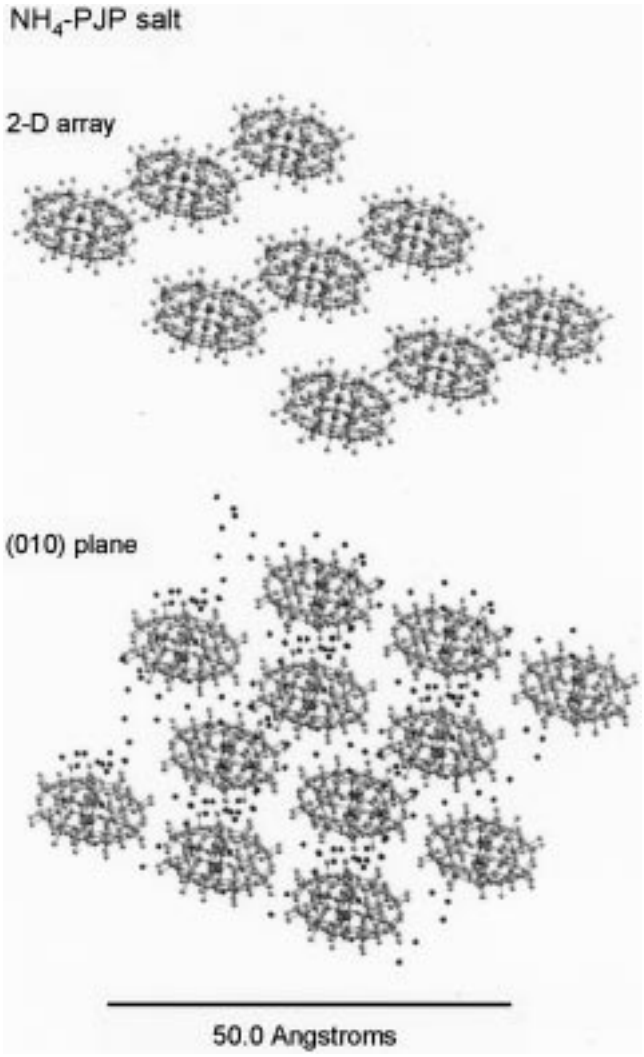

Figure 13. Comparison of POM anion packings between model STM images of the $(NH_4)_{14}$ PJP salt and the (010) plane of the bulk structure of $(NH_4)_{14}[NaP_5W_{30}O_{110}]\cdot 31H_2O$. Dark, unattached spheres in the latter represent the positions of NH_4^+ countercations from XRD.[32] Positions of the water molecules are not shown.

salt are collinear, while those in both the 2-D arrays and bulk structure of the ammonium salt are not. This observation suggests that counterions can influence not only lattice spacing but also lattice symmetry in these 2-D arrays of polyoxometalates. Confirmation of such structural differences in bulk crystals of these salts awaits structure determination for potassium PJP crystals, but ample precedents exist among the crystal structures of less complex inorganic salts (e.g., NaCl vs CsCl).

Conclusions

STM was used successfully to image the shapes, packing, and orientation of four different polyoxometalates with anisotropic molecular structures: Keggin, Finke−Droege, Wells−Dawson, and Pope−Jeannin−Preyssler. In all cases, well-ordered 2-D array anion monolayers were prepared on HOPG surfaces with packing structures similar to but not identical with those observed in 3-D bulk crystals. The spatially resolved tunneling spectra provided evidence for both anion and countercation locations in the 2-D anion arrays. The image periodicities reflected both the POM anion van der Waals dimensions and the presence of cations located between the POM anions in a manner consistent with the tunneling spectroscopy measurements. These results indicate that the formation of ordered monolayers by polyoxometalates can be generalized beyond the pseudospherical Keggin structure considered in previous studies, to include highly anisotropic POMs.

Acknowledgment. The authors gratefully acknowledge Drs. George Coulston and Dino Kourtakis of DuPont for providing the WD anion sample and Dr. Raul Lobo and Jim Rekoske of the Department of Chemical Engineering at the University of Delaware for their assistance in generating the structure simulations. Funding for this research was provided by the National Science Foundation (Grants CTS-9410965 to M.A.B. and CHE-9412465 to C.L.H.), and the TopoMetrix TMX 2010 STM instrument was acquired via an equipment grant from the U.S. Department of Energy.

Supporting Information Available: Fourier transform infrared spectra obtained by deposition of the following polyoxometalate samples on the diamond probe of a total internal reflectance spectrometer (Applied Systems, Inc., React IR model 1000): Keggin, $H_3[PW_{12}O_{40}]$; Pope−Jeannin−Preyssler, $(NH_4)_{14}[NaP_5W_{30}O_{110}]$; Finke−Droege, $Na_{16}[Cu_4(P_2W_{15}O_{56})_2]$; Wells−Dawson, $H_7[P_2Mo_{17}VO_{62}]$ (4 pages). Ordering information is given on any current masthead page.

IC9705655